PHYSICAL MODELING OF IMPACTS: THEORY AND EXPERIMENTS ON CONTACT TIME AND SPECTRAL CENTROID

Federico Avanzini
Dept. of Information Eng.
University of Padova
Via Gradenigo 6/A
35131 Padova, Italy
e-mail: avanzini@dei.unipd.it

Davide Rocchesso
Dept. of Computer Science
University of Verona
Strada le Grazie 15
37134 Verona, Italy
e-mail: rocchesso@sci.univr.it

ABSTRACT

A model for physically based synthesis of collision sounds is discussed. Attention is focused on the properties of the non-linear contact force, and on the influence of the physical parameters on the perceptually salient sound features. First, the dependence of the contact time on the force parameters is established analytically and validated through numerical simulations. Then, the relation with the time-varying spectral centroid is discussed. As a result, a mapping between the physical parameters of the impact force and the acoustic parameters of the impact sound is proposed.

Keywords: Physical Modeling, Impacts, Contact Time, Spectral Centroid

1. INTRODUCTION

According to ecological acoustics [7], the physical properties involved in sound generation can be grouped into two broad categories: *structural invariants* specify individual properties of objects such as size, shape, material; *transformational invariants* characterize interactions between objects (e.g. collisions, frictions, etc.). Recent works [14] have shown that oversimplified physical models are able to convey information on structural invariants (shape, size and materials) and to synthesize "cartoon" sounding objects where these invariants can be controlled. In this paper attention is turned to some transformational invariants that are originated in collision events, namely the impact "hardness". Freed [6] has addressed this topic using non-synthetic sounds. We use a non-linear contact force model originally proposed by Hunt and Crossley [10], and we apply it to a very simple system where a lumped hammer strikes a lumped resonator. The basic properties of the model are investigated both analytically and experimentally. The simple structure we have chosen allows us to study the influence of physical parameters (hammer and resonator masses, elasticity and damping coefficients of the non-linear contact force) on the system behavior. The contact time and the time-varying spectral centroid are chosen as the perceptually salient aspects of the acoustics of impacts, and their dependence on physical parameters is studied both analytically and experimentally.

Although performed using elementary resonator models, this investigation can be helpful for improving existing contact models in more complex systems: one example is hammer-string interaction in piano models, where contact time is a key feature for sound quality. The well known Stulov model [15] for piano hammer felts provides a realistic description of hysteretic contact forces, and is successful in fitting real data. However, recent research by Giordano and Mills [8] has questioned to some extent its general validity, suggesting the need for further investigations on alternative piano hammer models.

2. PHYSICALLY-BASED IMPACT MODELS

2.1. Modeling approaches

Impact models have been widely studied in musical acoustics, mainly in relation with hammer-string interaction in the piano. If the contact area between the two colliding objects is assumed to be small (ideally, a point), the simplest model [9] states a polynomial dependence of the contact force f on the hammer felt compression x:

$$f(x(t)) = \begin{cases} k[x(t)]^{\alpha} & x > 0, \\ 0 & x \leq 0, \end{cases} \qquad (1)$$

The compression x at the contact point is computed as the difference between hammer and string displacements. Therefore, the condition $x > 0$ states that there is actual felt compression, while the complementary condition $x \leq 0$ says that the two objects are not in contact. The parameter k is the force *stiffness*, and the exponent α depends on the local geometry around the contact area. As an example, in an ideal impact between two spherical objects α takes the value 1.5. Typical experimental values in a piano hammer felt range from 1.5 to 3.5, with no definite trend from bass to treble.

More realistic models have to take into account the hysteresis effects involved in the interaction. As an example, it is known that the force-compression characteristic in a piano hammer exhibits a hysteretic behavior, such that

loading and unloading of the hammer felt are not alike. In particular, the dynamic force-compression characteristic is strongly dependent on the hammer normal velocity before collision. In order to account for these phenomena, Stulov [15] proposed an improved model where the contact force possesses history-dependent properties. The idea, which is taken from the general theory of mechanics of solids, is that the spring stiffness k in Eq. (1) has to be replaced by a time-dependent operator. Consequently, according to Stulov the contact force can be modeled as

$$f(x(t),t) = \begin{cases} k[1 - h_r(t)] * [x(t)^\alpha] & x > 0, \\ 0 & x \leq 0, \end{cases} \quad (2)$$

where $*$ stands for the continuous-time convolution operator, and $h_r(t) = \frac{\epsilon}{\tau} e^{-t/\tau}$ is a *relaxation function* that controls the "memory" of the material. In fact, by rewriting the convolution explicitly the Stulov force is seen to be:

$$f(x(t),t) = kx(t)^\alpha - \frac{\epsilon}{\tau} e^{-t/\tau} \int_0^t e^{\xi/\tau} x(\xi)^\alpha \, d\xi \quad (3)$$

for $x > 0$. The Stulov model has proved to be successful in fitting experimental data where a hammer strikes a massive surface, and the signals of force, acceleration, and displacement are recorded. Borin and De Poli [4] showed that the model can be implemented numerically without significant losses in accuracy, stability and efficiency with respect to the simpler model (1).

Useful results on impact modeling are also found from studies in robotics. Physical modeling of contact events is indeed a relevant issue in dynamic simulations of robotic systems, when physical contact with the environment is required in order for the system to execute its assigned task (for example, handling of parts by an industrial manipulator during assembly tasks, or manipulator collisions with unknown objects when operating in an unstructured environment). Marhefka and Orin [12] provide a detailed discussion of a collision model that was originally proposed by Hunt and Crossley [10]. Under the hypothesis that the contact surface is small, Hunt and Crossley proposed the following form for the contact force f:

$$f(x(t),v(t)) = \begin{cases} kx(t)^\alpha + \lambda x(t)^\alpha v(t) & x > 0, \\ 0 & x \leq 0, \end{cases} \quad (4)$$

where $v(t) = \dot{x}(t)$ is the compression velocity, and k and α are defined as above. The parameter λ is the force damping weight.

Equation (4) can be rewritten as

$$f(x(t),v(t)) = kx(t)^\alpha \left[1 + \mu v(t)\right] \qquad x > 0, \quad (5)$$

where $\mu = \lambda/k$ is a mathematically convenient term. Similarly to Eqs. (1) and (2), the value of the exponent α depends only on the local geometry around the contact surface. Note that the force model (4) includes both an elastic component kx^α and a dissipative term $\lambda x^\alpha v$. Moreover, the dissipative term depends on both x and v, and is zero for zero compression.

Marhefka and Orin have studied the following case: an idealized hammer, described as a lumped mass $m^{(h)}$, strikes a surface. The surface mass is assumed to be much greater than $m^{(h)}$, therefore the surface is assumed not to move during the collision. When the two objects collide, the hammer initial conditions are $x^{(h)}(0) = 0$ (hammer position) and $\dot{x}^{(h)}(0) = -v_{in}$ (hammer normal velocity before collision). Since the surface is assumed not to move, the hammer position and velocity relate to the compression and compression velocity through the equalities $x^{(h)}(t) = -x(t)$, $\dot{x}^{(h)}(t) = -v(t)$. The hammer trajectory is therefore described by the differential equation $m^{(h)}\ddot{x}^{(h)} = f(-x^{(h)}, -\dot{x}^{(h)})$. Then it is shown in [12] that

$$\begin{aligned} \frac{d(\dot{x}^{(h)})}{dx^{(h)}} = \frac{\dot{v}}{v} = \frac{(\Lambda v + K)\,[x]^\alpha}{v}, \quad \Rightarrow \\ \int \frac{v\, dv}{(\Lambda v + K)} = \int [x]^\alpha \, dx, \end{aligned} \quad (6)$$

where two auxiliary parameters $\Lambda = -\lambda/m^{(h)}$ and $K = -k/m^{(h)}$ have been introduced for clarity. The integral in Eq. (6) can be computed explicitly and gives

$$x(v) = \left[\left(\frac{\alpha+1}{\Lambda^2} \right) \left(\Lambda(v - v_{in}) - K \log \left| \frac{K + \Lambda v}{K + \Lambda v_{in}} \right| \right) \right]^{\frac{1}{\alpha+1}}. \quad (7)$$

Equation (7) provides x as a function of v, and can therefore be exploited for plotting the phase portrait on the (x, v) plane. This is shown in Fig. 1(a).

Another remark by Marhefka and Orin is concerned with "stickiness" properties of the contact force f. From Eq. (4), it can be seen that f becomes inward (or sticky) if $v < v_{lim} := -1/\mu$. However, this limit velocity is never exceeded on a trajectory with initial conditions $x = 0$, $v = v_{in}$, as shown in the phase portrait of Fig. 1(a). The upper half of the plot depicts the trajectories of a hammer which strikes the surface with various normal velocities (trajectories are traveled in clockwise direction). Note that the output velocities after collision v_{out} are always smaller in magnitude than the corresponding v_{in}. Moreover, for increasing v_{in} the resulting v_{out} converges to the limit value v_{lim}. The horizontal line $v = v_{lim}$ corresponds to the trajectory where the elastic and dissipative terms cancel, and therefore the hammer travels from right to left with constant velocity. This horizontal line separates two regions of the phase space, and the lower region is never entered by the upper paths. The lower trajectories are entered for an initial compression $x > 0$ and initial *negative* compression velocity $v_{in} < v_{lim}$. If such conditions are imposed, then one of the lower trajectories is traveled from right to left: the hammer bounces back from the surface, while its velocity decreases in magnitude, due to the dissipative term in the force f.

Figure 1(b) shows the compression-force characteristics during collision. Note that the dissipative term $\lambda x^\alpha v$ introduces hysteresis. In this respect, the role of the dissi-

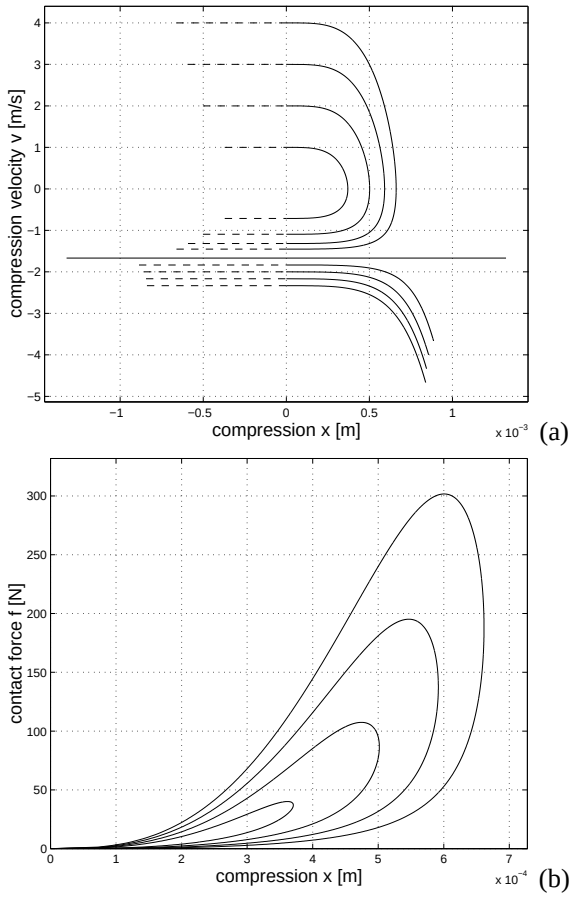

Figure 1. *Collision of a hammer with a massive surface for various v_{in}'s; (a) phase portrait, (b) compression-force characteristics. Values for the hammer parameters are $m^{(h)} = 10^{-2}$ [Kg], $k = 1.5 \cdot 10^{11}$ [N/m$^\alpha$], $\mu = 0.6$ [s/m], $\alpha = 2.8$, $v_{in} = 1 \dots 4$ [m/s].*

pative term in the Hunt and Crossley model is very similar to that of the relaxation function in the Stulov model

2.2. An exciter-resonator model

The Hunt and Crossley impact model (4) can be used as a coupling mechanism between two modal resonators. For clarity, the two objects are denoted with the superscripts (h) and (r), which stand for "hammer" and "resonator", respectively. The two objects interact through the contact force $f(x, v)$ given in Eq. (4).

According to modal analysis, the two resonators are described through a set of decoupled equations in which the variables $x_j^{(r,h)}$ are referred to as *modal displacements*. Each mode follows a second-order oscillator equation. Assuming the two resonating objects have $N^{(r)}$ and $N^{(h)}$ modes, respectively, their displacements at a given point k are given by a linear combination of the modal displacements: $\sum_{j=1}^{N^{(r,h)}} t_{kj}^{(r,h)} x_j^{(r,h)}$. Assuming that the interaction occurs at point $l = 1 \dots N^{(h)}$ of the hammer and point $m = 1 \dots N^{(r)}$ of the resonator, the continuous-time equations of the coupled system are given by:

$$
\begin{cases}
\ddot{x}_i^{(h)} + g_i^{(h)} \dot{x}_i^{(h)} + \left[\omega_i^{(h)}\right]^2 x_i^{(h)} = \dfrac{1}{m_{il}^{(h)}} (f_e^{(h)} + f) \\
\quad (\text{for} \quad i = 1 \dots N^{(h)}) \\
\ddot{x}_j^{(r)} + g_j^{(r)} \dot{x}_j^{(r)} + \left[\omega_j^{(r)}\right]^2 x_j^{(r)} = \dfrac{1}{m_{jm}^{(r)}} (f_e^{(r)} - f) \\
\quad (\text{for} \quad j = 1 \dots N^{(r)}) \\
x = x_{m,l} = \sum_{j=1}^{N^{(r)}} t_{mj}^{(r)} x_j^{(r)} - \sum_{i=1}^{N^{(h)}} t_{li}^{(h)} x_i^{(h)}, \\
v = v_{m,l} = \sum_{j=1}^{N^{(r)}} t_{mj}^{(r)} \dot{x}_j^{(r)} - \sum_{i=1}^{N^{(h)}} t_{li}^{(h)} \dot{x}_i^{(h)}, \\
f(x, v) = \begin{cases} k x^\alpha + \lambda x^\alpha \cdot v, & x > 0, \\ 0, & x \le 0, \end{cases}
\end{cases}
\tag{8}
$$

where the parameters $\omega^{(r,h)}$ and $g^{(r,h)}$ are the oscillator center frequencies and damping coefficients, respectively. The parameters $1/m^{(r,h)}$ control the "inertial" properties of the oscillators (note that $m^{(r,h)}$ has the dimension of a mass). The terms $f_e^{(h)}, f_e^{(r)}$ represent external forces.

As a special case, one or both the objects can be an inertial mass, described with one mode, zero spring constant and zero internal damping. As another special case, one object can be a "rigid wall", i.e. a modal object with an ideally infinite mass.

The continuous-time system (8) is discretized using the bilinear transformation [13] (also known as the one-step *Adams-Moulton* method [11] in the numerical analysis literature). The bilinear transformation is one appealing discretization technique for various reasons. First, its order of accuracy can be seen [11] to be two. Second, the transformation preserves the order of the system. Finally, the transformation is stable, since the left-half s-plane is mapped into the unit z-circle. Consequently, the bilinear transformation provides a reasonable trade-off between accuracy and efficiency.

After applying the bilinear transformation to system (8), the resulting discrete-time system appears as a parallel bank of second-order low-pass resonant filters, each one accounting for one specific mode of the resonator.

It can be seen that, being the bilinear transformation an implicit method, the variables $[x(n), v(n)]$ and $f(n)$ have instantaneous mutual dependence at each time step n. That is, a delay-free non-computable loop has been created in the discrete-time equations, and since a non-linear term is involved in the computation, the loop cannot be easily rearranged into a computable structure. This is a known problem in numerical simulations of non-linear dynamic systems. An accurate and efficient solution, called K method, has been proposed in [3] and is adopted here. Details about the discrete-time system have been discussed elsewhere [14] and will not be addressed in this paper.

3. CONTACT TIME

In this section we derive an equation that relates the contact time t_0 (i.e. the time after which the hammer sepa-

rates from the struck object) to the physical parameters of the contact model. The details of the derivation have been extensively discussed elsewhere [1, 2], here only the main steps are summarized.

The contact time has a major role in defining the spectral characteristics of the initial transient. Qualitatively, a short t_0 corresponds to an impulse-like transient with a rich spectrum, and thus provides a bright attack. Similarly, a long t_0 corresponds to a smoother transient with little energy in the high frequency region. Therefore t_0 influences the spectral centroid of the attack transient. It is known that the spectral content of the attack transient determines to a large extent the perceived quality of the impact. In a study on perceived mallet hardness, Freed [6] found that the perception of hardness is strongly correlated to the spectral centroid of the attack transient.

Hunt and Crossley [10] found an expression for the normal velocity after collision v_{out} in the limit of small μ (a similar discussion is also reported in [12]). In this limit the relation $v_{out} = (-1 + \frac{2}{3}\mu)v_{in}$ is found, in which the *coefficient of restitution* has a linear dependence on the parameter μ. In the general case (i.e., when the parameter μ is allowed to take non-small values), studying the behavior of v_{out} is less trivial, and Hunt and Crossley do not address this case.

The velocities v_{in} and v_{out} correspond to the points where $x_h = 0$, i.e. to the roots of the right-hand side in Eq. (7). Therefore, from Eq. (7) v_{out} is found as

$$\begin{aligned} & x_h(v_{out}) = \Lambda(v_{out} - v_{in}) - K \log \left| \frac{K + \Lambda v_{out}}{K + \Lambda v_{in}} \right| = 0, \\ \Rightarrow \quad & \frac{e^{\mu v_{out}}}{1 + \mu v_{out}} = \frac{e^{\mu v_{in}}}{1 + \mu v_{in}}. \end{aligned} \tag{9}$$

This equation shows that v_{out} depends only on μ and the input velocity v_{in} even in the general case. A graphic study of the function $e^{\mu v}/(1 + \mu v)$, as given in Fig. 2(a), provides a qualitative description of the dependence $v_{out}(v_{in})$. It is seen that $v_{out} \to v_{lim}$ for $v_{in} \to \infty$, consistently with the phase portrait in Fig. 1.

The second Eq. (9) can be rewritten as

$$e^{\mu v_{out}} = a\,(1 + \mu v_{out})\,, \text{ where } a = \frac{e^{\mu v_{in}}}{1 + \mu v_{in}}. \tag{10}$$

Therefore v_{out} is the intersection of the exponential on the left-hand side and the linear function on the right-hand side, as shown in Fig. 2(b). The velocity v_{out} can be found numerically as the root of Eq. (10).

Having v_{out}, the contact time t_0 can now be computed. If collision occurs at $t = 0$, then the contact time is by definition given by $t_0 = \int_0^{t_0} dt$. Moreover, since $dt = dx_h/v$, also by definition, it is easily seen from Eq. (6) that

$$\begin{aligned} dt = \frac{dx_h}{v} = \frac{dv}{(\Lambda v + K)x_h^\alpha}, \quad & \Rightarrow \\ t_0 = \int_0^{t_0} dt = \int_{v_{in}}^{v_{out}} & \frac{dv}{(\Lambda v + K)x_h^\alpha}. \end{aligned} \tag{11}$$

Recalling Eq. (7), x^α can be rewritten in the integral as a function of the velocity v. Thus, the integrand function

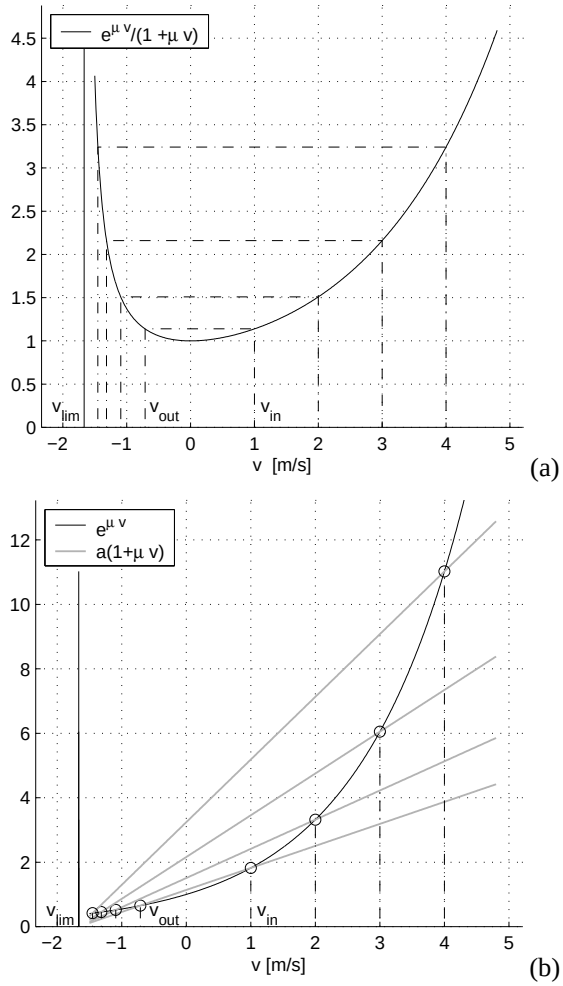

Figure 2. *Graphic study of v_{out} for various v_{in}'s. Values for the parameters are the same used in Fig. 1.*

depends only on v. Then straightforward calculations lead to the expression

$$t_0 = \left(\frac{m^{(h)}}{k}\right)^{\frac{1}{\alpha+1}} \cdot \left(\frac{\mu^2}{\alpha+1}\right)^{\frac{\alpha}{\alpha+1}} \cdot \int_{v_{out}}^{v_{in}} \frac{dv}{(1+\mu v)\left[-\mu(v - v_{in}) + \log\left|\frac{1+\mu v}{1+\mu v_{in}}\right|\right]^{\frac{\alpha}{\alpha+1}}}. \tag{12}$$

It can be checked that the constant outside the integral has dimension [s^2/m], while the integral itself is a velocity [m/s]. Therefore, the whole expression on the right-hand side has dimension [s].

Equation (12) states that the contact time t_0 depends only on μ, the exponent α, and the ratio $m^{(h)}/k$ (plus the impact velocity v_{in}). Note that, for a given value of α, the constant outside the integral depends only on μ and the ratio $m^{(h)}/k$. Since neither $m^{(h)}$ nor k affect the value of the integral (recall that v_{out} depends only on μ and v_{in}), it follows that the power-law dependence $t_0 \sim (m^{(h)}/k)^{1/(\alpha+1)}$ holds. The dependence $t_0(\mu)$ is less easily established analytically; however, numerical

integration of Eq. (12) can be used in order to study such dependence. Note that the singularities at v_{out}, v_{in} require additional care while integrating near the boundaries.[1]

The influence of the model parameters on the contact time has been analyzed experimentally [2, 1], in order to validate equation (12). Here we summarize the results.

Two types of numerical experiments were performed. In a first setup the hammer strikes a rigid surface and rebounds from it (this is the same setting used in Sec. 3 for deriving Eq. (12)). A second experimental setup involves collision between the non-linear hammer and the resonator described in Sec. 2.2. Several simulations were run in which the parameters were varied over a large range and the contact time t_0 was computed and compared with the values resulting from numerical integration of Eq. (12). One notable result from numerical experiments is that the contact time varies very slowly with μ, while $m^{(h)}/k$ and α have a stronger influence on t_0. When the hammer collides with a resonating object, an additional dependence of t_0 on the resonator parameters is introduced. Experimentally we observed that in this case t_0 is always higher than the value predicted by equation (12), due to the compliance of the struck object.

4. SPECTRAL CENTROID

In section 3 we have stated that the contact time has a major role in defining the spectral characteristics of the initial transient of an impact sound. This section provides an original quantitative assessment of this statement.

The exciter-resonator model summarized in system (8) was used as a numerical experimental testbed. The simulations described in the remainder of this section were performed using the following settings.

- Hammer: $N^{(h)} = 1, \omega_1^{(h)} = 0, g_1^{(h)} = 0$, i.e., the "hammer" was described as an inertial mass without resonating modes.

- Resonator: $N^{(r)} = 3, [\omega_j^{(h)}] = 2\pi f_0[1, (5/3.011)^2, (7/3.011)^2]$ (i.e. the resonator was given 3 resonating modes tuned to those of an ideal bar with free edges [5]; f_0 is the pitch), and $g_j^{(r)} = \omega_j/q$, where q is the quality factor of the second-order oscillators.

Using these settings, simulations were run in which the physical parameters of the impact force $(m^{(h)}, k, \mu, \alpha)$ were varied on a wide range. For each simulation, the contact time and the time-varying centroid in the first 100ms were computed.

The results are summarized in figure 3. Each row reports the results for one of the four parameters. The plots in the first column depict the contact time as a function of the varying parameter, and are in accordance with previously established results [1, 2]. Note in particular that the contact time is almost independent on μ.

The plots in the second column of figure 3 depict the spectral centroid as a function of time (first 100ms) and of the varying parameter (the arrow indicates the direction of increase of the parameter). The centroid was computed on 1024 sample DFT (i.e., a $\sim$ 23ms time window, with a 44.1kHz sampling rate). A clear correlation between the contact time and the spectral centroid can already be noticed: as the contact time increases, the initial "bump" in the resulting sound is lenghtened and correspondingly the centroid estimation is lowered. For sufficiently long contact times, the estimated centroid becomes lower than the resonator pitch f_0: see in particular the plots in the first and fourth rows of figure 3. An example of initial transients with short and long contact times is given in figure 4(a).

The plots in the third column of figure 3 depict the average c_{av} of the spectral centroid (first 100ms) as a function of the contact time, and illustrate more clearly the correlation between the two parameters. Note that the parameter μ has an effect on the centroid even though the contact time remains approximately constant. This effect is illustrated in figure 4(b): as μ is lowered, the amount of energy transferred to the higher partials during contact is increased, and the centroid increases accordingly. Similarly, note that the centroid increases significantly for low values of α, even though the contact time varies slowly. This effect is illustrated in figure 4(c): as α is lowered, the impact force increases significantly and eventually produces multiple bounces of the resonator on the hammer, with a consequent increase of the centroid. This effect also explains the non monotonicity of the contact time–centroid curve for low α values.

5. DISCUSSION

The discussion in sections 3 and 4 about the influence of the physical parameters on contact time and spectral centroid have shown in particular that

- The contact time is almost independent on the dissipative component of the contact force.

- The centroid is strongly correlated to the contact time, but depends also on the dissipative component of the contact force.

These results can be exploited to derive a mapping between the physical parameters of the contact force and the sound features. Given an exciter-resonator system, and given the hammer mass $m^{(h)}$ and force exponent α, the results outlined in sections 3 and 4 can be used to derive a mapping $(k, \mu) \mapsto (t_0, c_{av})$.

As a first approximation, a linear regression on the experimental data can be tried. Figure 5 shows the linear fits for the $t_0(k)$, $c_{av}(k)$, and $c_{av}(\mu)$ curves (logarithmic scales). By using these linear fits, the control mapping

[1] The integrand function has two singularities at v_{out} and v_{in}. However, it can be checked that at these boundaries the integrand function converges asymptotically to $1/(v - v_{out})^{\alpha/(\alpha+1)}$ and $1/(v - v_{in})^{\alpha/(\alpha+1)}$, respectively. Therefore the integral takes finite values for any $\alpha > 0$.

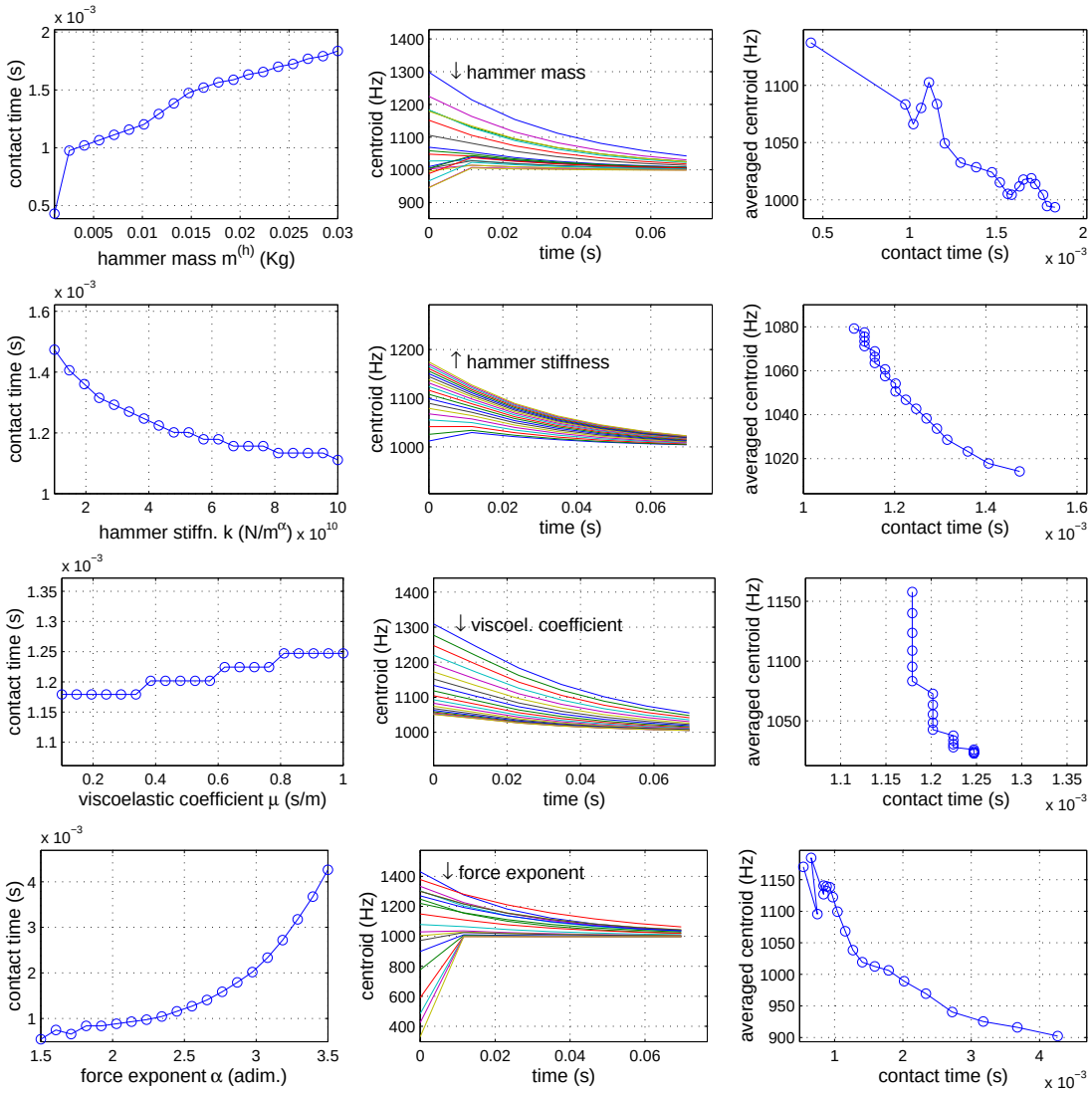

Figure 3. *Spectral centroid analysis. Left plots: dependence of t_0 on the impact force parameters. Center plots: dependence of the spectral centroid on the impact force parameters. Right plots: spectral centroid mean (first 100 ms) vs contact time. When not varying, the force parameters have values $m^{(h)} = 1 \cdot 10^{-3}$Kg, k=$5 \cdot 10^{10}N/m^{\alpha}$, $\mu = 0.5$s/m, $\alpha = 2.5$. The resonator pitch is $f_0 = 1000$Hz.*

$(k, \mu) \mapsto (t_0, c_{av})$ can be defined to be an 2D affine transformation:

$$\begin{bmatrix} t_0 \\ c_{av} \end{bmatrix} = \begin{bmatrix} a_{1,1} & 0 \\ a_{2,1} & a_{2,2} \end{bmatrix} \cdot \begin{bmatrix} k \\ \mu \end{bmatrix} + \begin{bmatrix} t_{0,0} \\ c_{av,0} \end{bmatrix}. \quad (13)$$

Inversion of this equation results in a perceptually-motivated control mapping, in which the parameters (k, μ) of the physical model are determined on the basis of the sound features (t_0, c_{av}).

More rigorous investigations are needed in order to assess the perceptual relevance of the selected acoustic parameters and the salience of the proposed mapping (13). In particular, listening tests should be performed using auditory stimuli synthesized with the proposed model, in order to investigate quantitatively the role of contact time and spectral centroid on the perceived hammer hardness.

Acknowledgment

This research was partially supported by the EU Sixth Framework Programme – IST Information Society Technologies (Network of Excellence "Enactive Interfaces" IST-1-002114, http://www.enactivenetwork.org).

6. REFERENCES

[1] F. Avanzini. *Computational Issues in Physically-based Sound Models*. PhD thesis, Dept. of Information Engineering, Univ. of Padova, Italy, 2001. Available at `http://www.dei.unipd.it/~avanzini`.

[2] F. Avanzini and D. Rocchesso. Modeling collision sounds: Non-linear contact force. In *Proc. COST-*

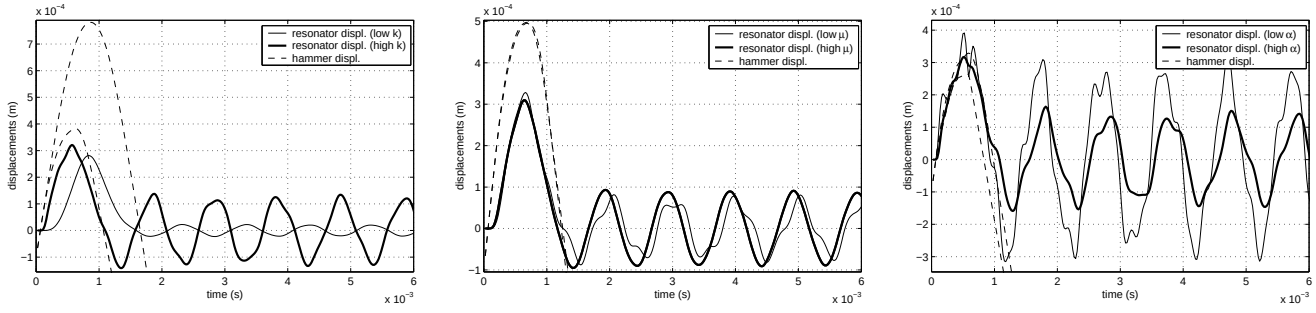

(a) (b) (c)

Figure 4. *Examples of transient attacks obtained from the impact model. (a) short vs. long initial bumps obtained by varying the force stiffness k; (b) varying amount of energy transferred to the higher partials obtained by varying the force parameter μ; (c) single vs. multiple contacts obtained by varying the exponent α.*

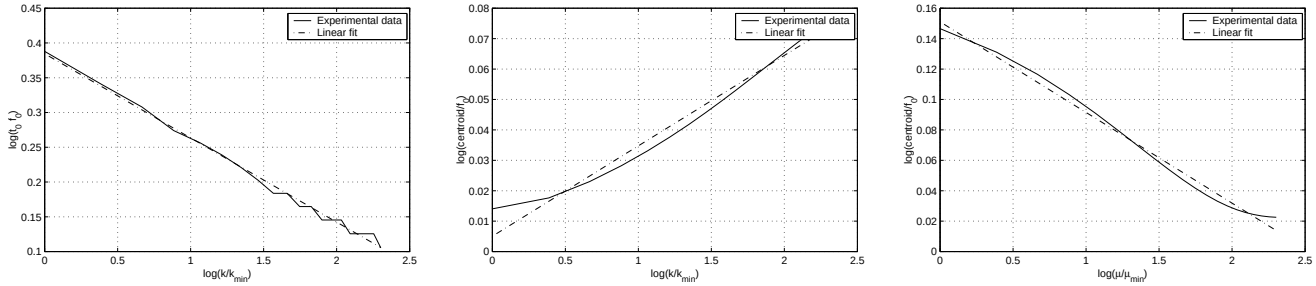

(a) (b) (c)

Figure 5. *Linear fits of the experimental data. (a) contact time t_0 vs. force stiffness k; (b) averaged centroid c_{av} vs. force stiffness k; (c) averaged centroid c_{av} vs. μ.*

G6 Conf. on Digital Audio Effects (DAFx01), pages 61–66, Limerick, Ireland, 2001.

[3] G. Borin, G. De Poli, and D. Rocchesso. Elimination of delay-free loops in discrete-time models of nonlinear acoustic systems. *IEEE Trans. Speech Audio Processing*, 8(5):597–606, 2000.

[4] G. Borin and G. De Poli. A hysteretic hammer-string interaction model for physical model synthesis. In *Proc. Nordic Acoustical Meeting*, pages 399–406, Helsinki, 1996.

[5] N. H. Fletcher and T. D. Rossing. *The Physics of Musical Instruments*. Springer-Verlag, NY, 1991.

[6] D. J. Freed. Auditory Correlates of Perceived Mallet Hardness for a Set of Recorded Percussive Events. *J. Acoust. Soc. Am.*, 87(1):311–322, 1990.

[7] W. W. Gaver. How Do We Hear in the World? Explorations in Ecological Acoustics. *Ecological Psychology*, 5(4):285–313, 1993.

[8] N. Giordano and J. P. Mills. Hysteretical Behavior of Piano Hammers. In *(ISMA'01)*, pages 237–241, Perugia, 2001.

[9] D. E. Hall. Piano string excitation VI: Nonlinear modeling. *J. Acoust. Soc. Am.*, 92:95–105, 1992.

[10] K. H. Hunt and F. R. E. Crossley. Coefficient of Restitution Interpreted as Damping in Vibroimpact. *ASME J. Applied Mech.*, pages 440–445, 1975.

[11] J. D. Lambert. *Numerical Methods for Ordinary Differential Systems*. John Wiley & Sons, Chichester, UK, 1993.

[12] D. W. Marhefka and D. E. Orin. A Compliant Contact Model with Nonlinear Damping for Simulation of Robotic Systems. *IEEE Trans. Systems, Man and Cybernetics-Part A*, 29(6):566–572, 1999.

[13] S. K. Mitra. *Digital Signal Processing: A computer-Based Approach*. McGraw-Hill, New York, 1998.

[14] D. Rocchesso and F. Fontana, editors. *The Sounding Object*. Mondo Estremo, Firenze, Italy, 2003. <http://www.soundobject.org>.

[15] A. Stulov. Hysteretic Model of the Grand Piano Hammer Felt. *J. Acoust. Soc. Am.*, 97(4):2577–2585, 1995.